Base-Catalysis of Imino Proton Exchange in DNA: Effects of Catalyst upon DNA Structure and Dynamics

Ewa Folta-Stogniew and Irina M. Russu*

Department of Molecular Biology and Biochemistry, Wesleyan University, Middletown, Connecticut 06459-0175

Received December 12, 1995; Revised Manuscript Received April 3, 1996[⊗]

ABSTRACT: Characterization of the kinetics and energetics of base-pair opening in nucleic acids relies upon measurements of the rates of exchange of imino protons with water protons at high concentrations of the exchange catalyst. Under these conditions, the exchange catalyst may affect structural or dynamic properties of the nucleic acid molecule and thus, limit the significance of the exchange data. To address this problem, we have used NMR spectroscopy to characterize the effects of a catalyst of imino proton exchange, namely, ammonia upon the structure and dynamics of the self-complementary DNA dodecamer $[d(CGCAGATCTGCG)]_2$. The changes in structure were monitored in proton NOESY and DQF-COSY experiments and in phosphorus spectra at 15 °C and at ammonia concentrations ranging from 0.002 to 0.5 M. The results indicate that ammonia induces subtle changes in the solution conformation of the dodecamer, but the overall structure is maintained close to the B-type DNA structure. However, the relaxation rates (i.e., transverse, longitudinal, and cross-relaxation rates) of several non-exchangeable protons were found to increase by ∼50% upon changing ammonia concentration from 0.002 to 0.5 M. The increases were comparable for all protons investigated suggesting that they originate from an ammonia-induced increase in the overall correlation time of the DNA dodecamer. Numerical analysis revealed that the catalyst-induced enhancements in proton relaxation can alter significantly the calculated values of the exchange rates of imino protons, especially those obtained from measurements of the line widths of these proton resonances.

Proton exchange measurements on nucleic acids have established that the exchange kinetics of Watson−Crick imino protons is a sensitive indicator of the fluctuations and transient opening of individual base pairs (Early et al., 1981; Pardi et al., 1982; Patel et al., 1983; Englander & Kallenbach, 1984; Cheung et al., 1984). The potential of these measurements for studies of structure−dynamics relationships in nucleic acids has been first demonstrated by Englander and co-workers using hydrogen isotope exchange (Teitelbaum & Englander, 1975a,b; Mandal et al., 1979; Englander & Kallenbach, 1984). These authors have shown that the exchange of imino protons requires formation of an open state of the base pair in which the imino proton is freed from its hydrogen bond and is accessible to the base that catalyzes the exchange. In these earlier studies, imino proton exchange rates were found to be unaffected by phosphate or other exchange catalysts. Thus, it was concluded that the exchange is limited only by the base-pair opening reaction, and the exchange rates provide a direct measure of the rates of base-pair opening. Recent experiments have demonstrated that this is not the case: the exchange of imino protons in nucleic acids can be greatly accelerated by addition of efficient catalysts such as Tris or ammonia (Leroy et al., 1985a,b, 1988; Gueron et al., 1987, 1990; Leontis & Moore, 1986). These observations indicated that, under usual buffer conditions (such as 10 mM phosphate at pH 7.0), the exchange is limited by the rate of abstraction of the imino proton by the base catalyst from the open state of the base pair. The opening-limited regime for imino proton exchange kinetics can be reached only in the presence of high concentrations of efficient base catalysts. Accordingly, the base-pair opening rates are derived by extrapolation of imino proton exchange rates to infinite catalyst concentration. They range from ∼10 to > 1000 s^{-1} at room temperature (Leroy et al., 1988; Gueron et al., 1990; Kochoyan et al., 1990; Moe & Russu, 1990, 1992; Folta-Stogniew & Russu, 1994). Similarly, the equilibrium constants for formation of the open state of base pairs are of the order of 10^{-5}−10^{-7}.

The high concentrations of base catalyst required to approach the opening-limited regime for imino proton exchange (i.e., up to ∼1 M) may be expected to alter the structure of a nucleic acid molecule. This raises an important question regarding the validity of the method and may limit the significance of the information derived from imino proton exchange. To address this question, in the present work, we have characterized the effects of a catalyst of imino proton exchange upon the conformation and motional properties of the dodecamer $[d(CGCAGATCTGCG)]_2$. The catalyst chosen for this study is ammonia. Due to its small size and high pK_a value, ammonia catalyzes the exchange of imino protons in DNA very efficiently (Gueron et al., 1990) and thus, it is widely used in measurements of base-pair opening. The kinetics and energetics of base-pair opening in the dodecamer $[d(CGCAGATCTGCG)]_2$ have been previously characterized by this laboratory (Folta-Stogniew & Russu, 1994).

EXPERIMENTAL PROCEDURES

Materials. The DNA dodecamer was synthesized on an Applied Biosystems synthesizer (model 381A) using the solid-support phosphoramidite method. The oligomer was

* Author to whom correspondence should be addressed.
[⊗] Abstract published in *Advance ACS Abstracts,* June 1, 1996.

S0006-2960(95)02932-1 CCC: $12.00

purified by reverse-phase high-pressure liquid chromatography on a PRP-1 column (Hamilton) in 50 mM ethylenediamine formate buffer, pH 7.5, with a gradient of 0−12.5% acetonitrile over 25 min. The counterions were exchanged to sodium by extensive dialysis against 0.6 M NaCl. The DNA samples were obtained by dialysis against deuterated ammonia buffers. All ammonia buffers used in the experiments contained 100 mM NaCl and 2 mM EDTA (pH-meter reading 8.9 at 25 °C).

For one-dimensional (1D)[1] ^{1}H NMR experiments, two samples of equal DNA concentration (1 mM duplex) were prepared in 0.002 and 0.5 M ammonia buffers, respectively. Intermediate concentrations of ammonia (i.e., 0.002, 0.05, 0.1, 0.25, and 0.5 M) were obtained by titrating the sample in 0.002 M ammonia with the sample in 0.5 M ammonia. For two-dimensional (2D) ^{1}H NMR experiments, five different ammonia concentrations (the same as those in the 1D experiments) were obtained by titrating a DNA sample in 2 mM deuterated ammonia buffer with a stock solution of 3.65 M deuterated ammonia buffer containing 100 mM NaCl and 2 mM EDTA (pH-meter reading 8.9 at 25 °C). The DNA concentration (duplex) was 1.1 mM at the beginning of titration and 0.95 mM at the end.

For ^{31}P NMR experiments, two samples of equal DNA concentration (0.7 mM duplex) were prepared in 0.002 and 1.75 M ammonia buffers, respectively. Intermediate concentrations of ammonia were obtained by titrating the sample in 0.002 M ammonia with the sample of high ammonia concentration. Spectra were obtained at 14 different ammonia concentrations in the range from 0.002 to 0.5 M.

Proton longitudinal, transverse, and cross-relaxation rates were measured on two samples of the same DNA concentration (1 mM duplex) in 0.002 and 0.5 M deuterated ammonia buffers.

All NMR experiments reported in this study were carried out in deuterated ammonia buffers. In order to compare them with imino proton exchange measurements the isotopic effect on the ionization equilibria of ammonia must be known. We have measured this effect from pH-titration curves of 0.05 M ammonia solutions at 23 °C, in H_2O and D_2O, respectively. The pK_a value in deuterated solutions was found to be higher by 0.5 pH units than that in protonated solutions. This difference is comparable to the isotopic effect on the glass electrode (namely, pD = pH-meter reading + 0.4; Glasoe & Long, 1960). Thus, for the experiments reported in the paper (0.002−0.5 M deuterated ammonia), the concentration of ammonia base ranged from 0.0005 to 0.13 M. The corresponding range of base concentrations in an aqueous ammonia buffer is 0.0006−0.15 M [at pH = 8.9 at 25 °C (which corresponds to pH = 9.2 at 15 °C) and based on a pK_a value of 9.56 for aqueous ammonia at 15 °C (Weast, 1986)]. The concentrations of base catalyst used when measuring base-pair opening in DNA extend to ∼1 M. This upper range of ammonia concentrations was not accessible to our present investigation because, at ammonia concentrations higher than 0.5 M, the intensities of cross-peaks in the 2D spectra were very low due to resonance broadening (see Results).

[1] Abbreviations: NMR, nuclear magnetic resonance; 1D, one-dimensional; 2D, two-dimensional; NOESY, nuclear Overhauser effect spectroscopy; DQF-COSY, double-quantum filtered correlated spectroscopy; T_1, longitudinal relaxation time; T_2, transverse relaxation time.

Methods. The NMR experiments were carried out at 15 °C on a Varian VXR-400/54 spectrometer operating at 9.4 tesla. Proton spectra were referenced to 2,2-dimethyl-2-silapentane-5-sulfonate (DSS) as an external reference. Phosphorus spectra were referenced to an external 85% phosphoric acid standard. Phase-sensitive proton DQF-COSY and NOESY spectra in D_2O were obtained as described (Piantini et al., 1982; States et al., 1982). The NOESY spectra as a function of ammonia concentration were obtained at a mixing time of 100 ms.

Proton longitudinal relaxation times (T_1) were measured using the selective saturation−recovery method. Each resonance of interest was selectively saturated by a low-power decoupler pulse, and the return of the magnetization to equilibrium was followed during a subsequent recovery delay. Twelve values of the recovery delay were used for each measurement. The T_1 values were calculated by fitting the intensity of the resonance, $I(t)$, as a function of recovery delay, t, to the following equation:

$$I(t) = I^0 + [I(0) - I^0]\exp(-t/T_1)$$

where $I(0)$ is the resonance intensity immediately following the decoupler pulse [$I(0) \simeq 0$] and I^0 is the resonance intensity at equilibrium. Proton transverse relaxation times (T_2) were calculated from the line widths at half-height ($\Delta\nu_{1/2}$) of the resonance of interest from the equation

$$\Delta\nu_{1/2} = 1/(\pi T_2)$$

The errors in line width measurements were estimated from several series of independent measurements and were found to be 10% or less.

Proton cross-relaxation rates were measured from NOESY experiments with mixing times of 0, 50, 75, and 100 ms. Cross-peak volumes were normalized against the volume of an one-proton diagonal peak at a mixing time of 0 ms. The average volume of the diagonal peaks of T7-H6, A4-H8, and A6-H8 was used for normalization. The errors in measurements of cross-peak volumes were estimated as ±15%. The cross-relaxation rates were obtained from the relaxation equation

$$\frac{d\mathbf{A}(\tau_m)}{dt} = -\mathbf{R} \times \mathbf{A}(\tau_m) \quad (1)$$

using the following approximation:

$$A_{ij}(\tau_m) = -R_{ij}\tau_m + {}^1/_2 \sum_k R_{ik}R_{kj}\tau_m{}^2 \quad (2)$$

where $\mathbf{A}(\tau_m)$ is the matrix of diagonal and cross-peaks volumes, τ_m is the mixing time, and $\mathbf{R}$ is the relaxation matrix (Macura & Ernst, 1980). Experimental cross-peak volumes were fitted to eq 2 using a nonlinear least-squares program. Cross-relaxation rates, R_{ij} ($i \neq j$), were determined from the term linear in τ_m. The errors reported in the paper for cross-relaxation rates represent one standard deviation of the nonlinear least-squares fits.

RESULTS

Figure 1 illustrates the effects of ammonia on the 1D ^{1}H NMR spectrum of the dodecamer. Gradual broadening is observed for all resonances upon increasing ammonia

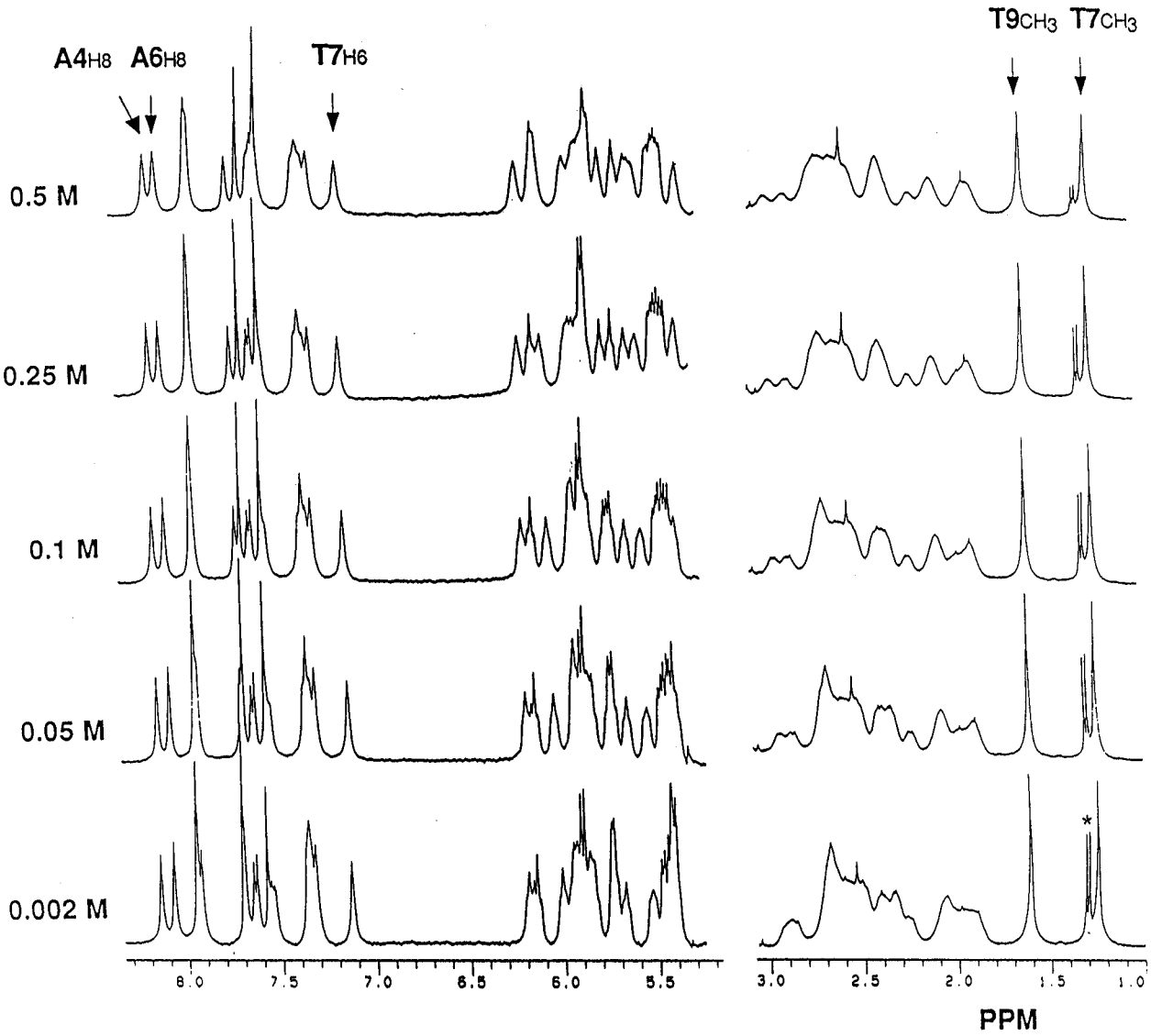

FIGURE 1: Selected regions of the ^{1}H NMR spectra of the dodecamer as a function of ammonia concentration at 15 °C. Solution conditions: ammonia buffer in D_2O with 100 mM NaCl and 2 mM EDTA, pH-meter reading 8.9 (at 25 °C). The proton resonances for which longitudinal and transverse relaxation rates were measured are indicated. The resonances indicated by the asterisk originate from an impurity in the buffer.

concentration. Moreover, the spectral positions of selected base and sugar proton resonances change upon increasing ammonia concentration, e.g., resonances between 7.5 and 8.0 ppm and between 5.3 and 6.3 ppm. The low resolution of 1D NMR spectra, particularly for sugar proton resonances, does not allow unique identification of these ammonia-induced changes in chemical shift. To overcome this limitation, we have carried out NOESY and DQF-COSY experiments at five ammonia concentrations in the range from 0.002 to 0.5 M. Assignments of all base and sugar protons (except H5′ and H5″) were obtained from NOESY experiments and confirmed, for scalar-coupled protons, from DQF-COSY experiments. Selected regions of the NOESY and DQF-COSY spectra at the lowest and highest ammonia concentrations investigated are shown in Figures 2 and 3, respectively (see also Chart 1 for numbering scheme). The ammonia-induced changes in the chemical shifts of proton resonances of the dodecamer are summarized in Figure 4.

Further evidence for the effect of ammonia upon the solution structure of the dodecamer was obtained from the volumes of cross-peaks in NOESY spectra. In order to remove any variations in NOESY cross-peak volumes due to changes in the correlation time (*vide infra*), the volumes of NOESY cross-peaks were scaled against the volume of the H5-H6 cross-peak of the cytosine in position 8 ($F1$ = 7.53 ppm and $F2$ = 5.48 ppm). A total of 53 cross-peaks were analyzed at each ammonia concentration. They represent H8/H6-H2′, H8/H6-H2″, H8/H6-H1′, H1′-H2′, and H1′-H2″ connectivities. The volumes of cross-peaks involving H3′ or H4′ sugar protons could not be measured accurately since they are affected by the large signal from residual water which, in ammonia buffer, cannot be reduced by repeated lyophilization. The ammonia-induced changes in NOESY cross-peak volumes are summarized in Figure 5.

The changes in sugar conformation were inferred from DQF-COSY experiments (Figure 3). The $^3J_{H1'-H2'}$ and $^3J_{H1'-H2''}$ coupling constants were measured for each nucleotide except G2 and G10 (for which the cross-peaks overlap) from the separation of in-phase and anti-phase components of the H1′-H2″ cross-peaks, as illustrated in Figure 3C. The sums $\sum_{1'}$ ($= {}^3J_{H1'-H2'} + {}^3J_{H1'-H2''}$) were measured from the separation of outer components in each cross-peak (Rinkel & Altona, 1987). The results are presented in Table 1. The measurements of scalar coupling constants from DQF-COSY

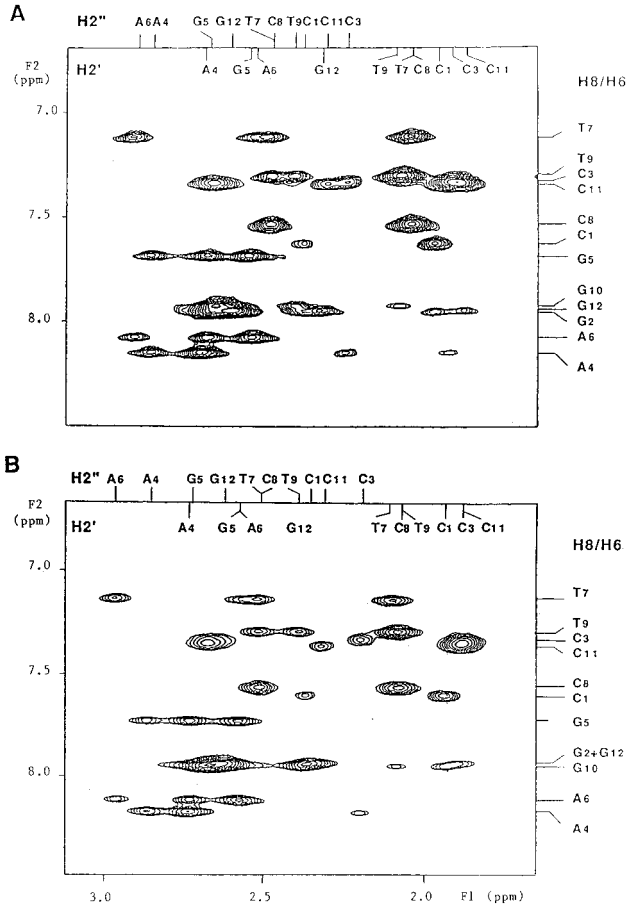

FIGURE 2: Expanded region of the NOESY spectra showing connectivities between base H8/H6 and sugar H2′/H2″ protons: (A) 0.002 M ammonia; (B) 0.5 M ammonia. Mixing time 100 ms. Solution conditions: ammonia buffer in D_2O with 100 mM NaCl and 2 mM EDTA, pH-meter reading 8.9 (at 25 °C). Assignments of resonances are indicated according to the numbering scheme shown in Chart 1 (resonances of H2′ and H2″ protons of G2 and G10 overlap and cannot be unambiguously assigned).

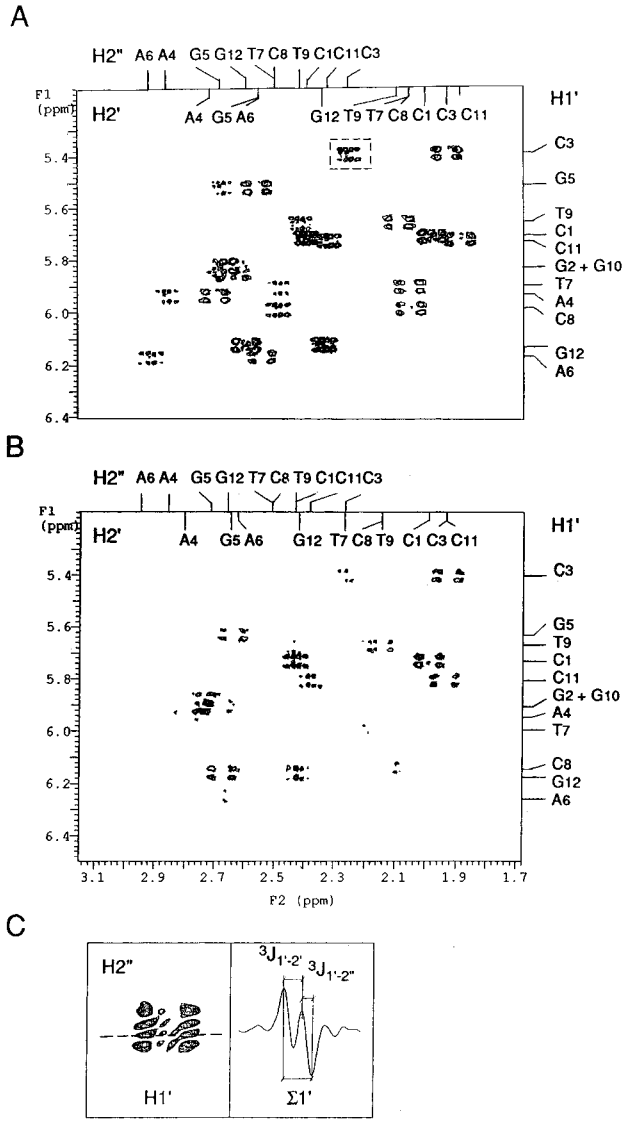

FIGURE 3: Expanded region of the DQF-COSY spectra showing connectivities between sugar H1′ and H2′/H2″ protons: (A) 0.002 M ammonia; (B) 0.5 M ammonia. Solution conditions: ammonia buffer in D_2O with 100 mM NaCl and 2 mM EDTA, pH-meter reading 8.9 (at 25 °C). Assignments of resonances are indicated according to the numbering scheme shown in Chart 1 (resonances of H2′ and H2″ protons of G2 and G10 overlap and cannot be unambiguously assigned). (C) Enlargement of the H1′-H2″ cross-peak of C3 (boxed in panel A) and the trace along H1′ frequency axis at position indicated by dashed line illustrating the measurement of the $^3J_{H1'-H2'}$ and $^3J_{H1'-H2''}$ coupling constants and the sum $\Sigma_{1'}$ ($= {}^3J_{H1'-H2'} + {}^3J_{H1'-H2''}$).

cross-peaks were possible only for the lower range of ammonia concentrations. At higher ammonia concentrations, the resonance line widths become comparable to or larger than the separation of multiplet components. As a result, the apparent separation of multiplet components does not reflect accurately the scalar coupling constants (Neuhaus et al., 1985). Moreover, the intensities of DQF-COSY cross-peaks are greatly reduced. For example, in 0.5 M ammonia, the only intense cross-peaks are those from terminal nucleotides (i.e., C1, G2, C3, G10, C11, and G12), and the cross-peaks of central nucleotides are barely visible (Figure 3B).

The gradual broadening of non-exchangeable proton resonances with increasing ammonia concentration suggested that ammonia affects the relaxation rates of the protons in the DNA dodecamer. To characterize this effect, we have measured the longitudinal and transverse relaxation rates for five non-exchangeable proton resonances, namely, A4-H8, A6-H8, T7-H6, T7-CH_3, and T9-CH_3 in 0.002 and 0.5 M ammonia solutions in D_2O. These resonances are the only proton resonances of the dodecamer that are well resolved at both ammonia concentrations (Figure 1). The results are shown in Table 2. We have also measured the cross-relaxation rates for several pairs of protons separated by a fixed distance, namely cytosine H5-H6 and thymine H6-CH_3. The NOESY build-up curves for these pairs of protons were

Chart 1. Numbering of Base Pairs in the Dodecamer Investigated

```
        1  2  3  4  5  6  7  8  9 10 11 12
5'-d(C  G  C  A  G  A  T  C  T  G  C  G) -  3'
3'- (G  C  G  T  C  T  A  G  A  C  G  C)d-  5'
       12 11 10  9  8  7  6  5  4  3  2  1
```

obtained in 0.002 and 0.5 M ammonia buffers from experiments with mixing times of 0, 50, 75, and 100 ms. The cross-relaxation rates were calculated based on eq 2 and are shown in Table 2C.

The changes in the phosphodiester backbone were monitored from ^{31}P spectra at fourteen ammonia concentrations in the range from 0.002 to 0.5 M. As shown in Figure 6A, increasing ammonia concentration results in uniform broad-

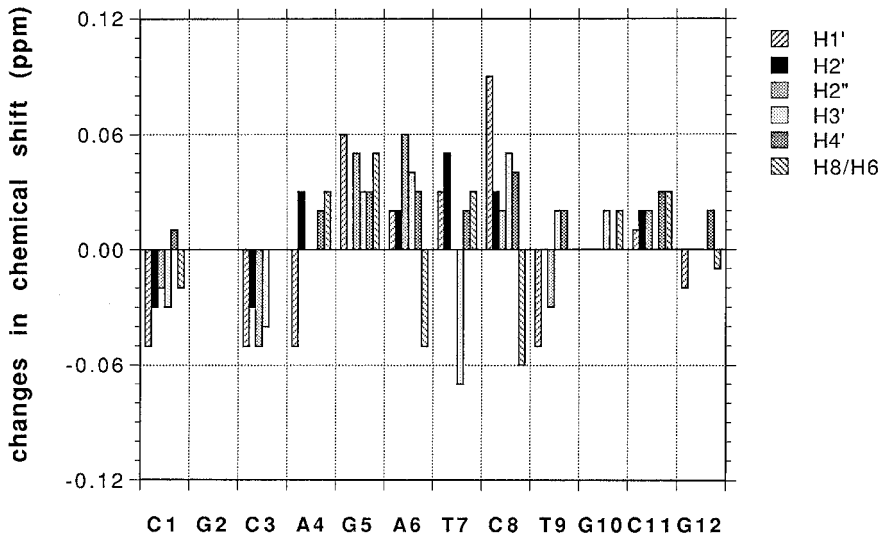

FIGURE 4: Ammonia-induced changes in the chemical shift of proton resonances of the dodecamer. The bars represent the differences in chemical shift at 0.002 and 0.5 M ammonia: δ(at 0.5 M) − δ(at 0.002 M). For other proton resonances, not included in the graph, the corresponding changes in chemical shift were −0.06 ppm for C8-H5, 0 ppm for C3-H5, 0.02 ppm for C8-H5, 0.04 ppm for C11-H5, 0.03 ppm for T7-CH_3, and 0 ppm for T9-CH3.

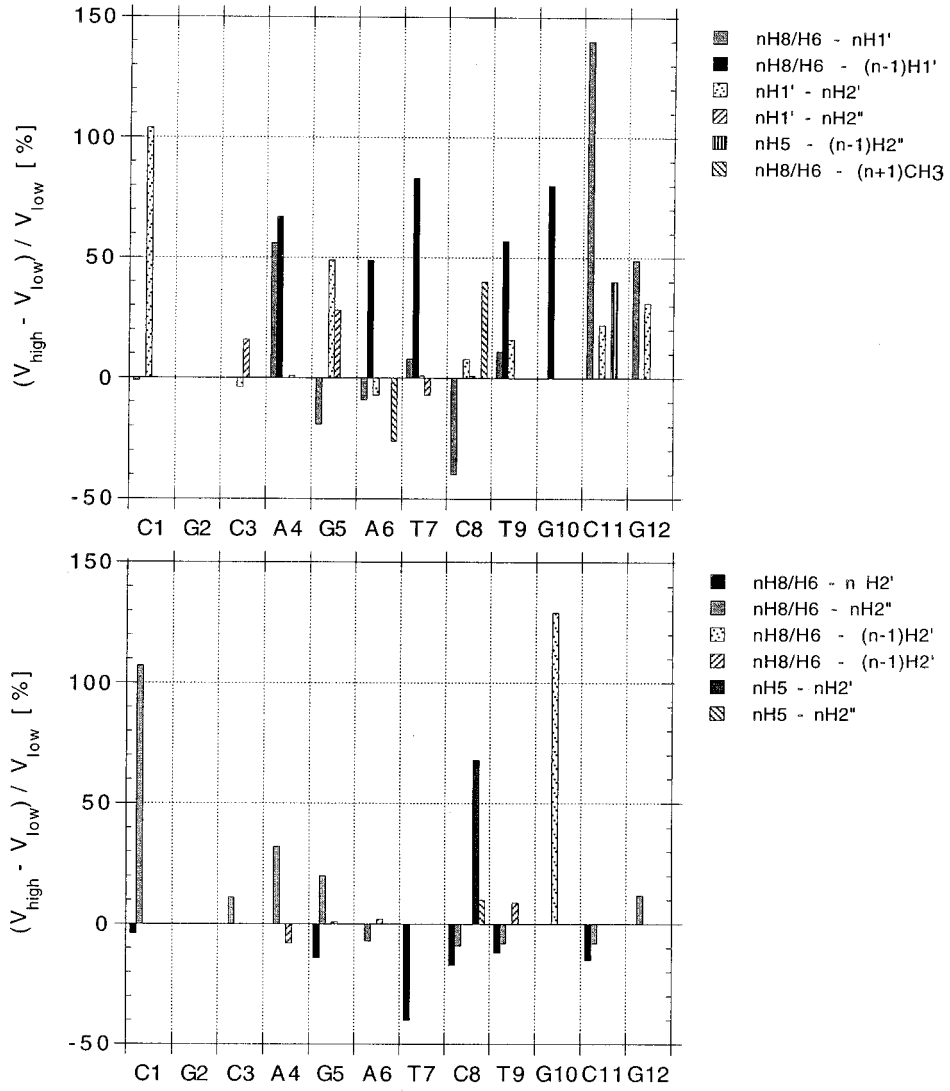

FIGURE 5: Relative changes in NOESY cross-peak volumes (mixing time 100 ms). The bars represent percentage increases (+) or decreases (−) in cross-peak volumes when the ammonia concentration is changed from 0.002 to 0.5 M. V_{low} and V_{high} are the volumes of a given cross-peak at 0.002 and 0.5 M ammonia concentration, respectively, scaled against the volume of the C8 H5-H6 cross-peak.

ening of the ^{31}P resonances of the dodecamer. Moreover, a few ^{31}P resonances in the region from −0.7 to −1.0 ppm shift upfield upon increasing ammonia concentration (Figure 6C).

Table 1: Scalar Coupling Constants as a Function of Ammonia Concentration at 15 °C

nucleotide	ammonia concentration (M) 0.002	0.05	0.1	0.25	0.5
	(A) $^3J_{H1'-H2'}$ (Hz)				
C1	9.3	8.6	9.3	9.2	10.0
G2	*a*	*a*	*a*	*a*	*a*
C3	9.8	9.6	9.7	*b*	*b*
A4	8.8	9.9	9.6	9.1	*b*
G5	*a*	9.9	10.4	*b*	*b*
A6	9.9	9.6	9.8	*b*	*b*
T7	9.8	9.3	10.3	*b*	*b*
C8	9.0	9.1	8.6	*b*	*b*
T9	8.7	9.4	8.9	9.0	*b*
G10	*a*	*a*	*a*	*a*	*a*
C11	9.2	8.7	9.0	10.3	9.4
G12	5.3	5.5	5.4	5.7	5.5
	(B) $^3J_{H1'-H2''}$ (Hz)				
C1	5.0	4.9	5.2	6.1	6.6
G2	*a*	*a*	*a*	*a*	*a*
C3	5.3	5.5	5.4	*b*	*b*
A4	5.3	5.6	5.0	5.3	5.5
G5	*a*	5.0	4.6	*b*	*b*
A6	5.7	5.7	6.2	*b*	*b*
T7	6.3	5.5	5.3	*b*	*b*
C8	6.0	5.6	5.3	*b*	*b*
T9	5.4	5.1	5.5	5.3	*b*
G10	*a*	*a*	*a*	*a*	*a*
C11	5.3	5.4	5.4	6.9	6.6
G12	9.4	9.6	9.2	9.5	9.4
	(C) $\sum 1' = {}^3J_{H1'-H2'} + {}^3J_{H1'-H2''}$ (Hz)				
C1	14.1	13.5	14.5	14.8	15.5
G2	*a*	*a*	*a*	*a*	*a*
C3	15.6	15.0	15.9	14.3	15.1
A4	14.1	16.3	15.6	14.3	*b*
G5	15.6	15.4	15.8	13.1	*b*
A6	14.3	15.7	13.9	15.3	*b*
T7	15.2	16.1	15.5	*b*	
C8	14.4	14.1	13.9	13.6	15.2
T9	14.7	15.0	15.4	14.3	13.7
G10	*a*	*a*	*a*	*a*	*a*
C11	14.2	14.3	14.3	15.2	15.2
G12	14.1	14.5	14.4	14.9	15.2

[a] Not measured due to the spectral overlap. [b] Unreliable measurements due to resonance broadening. The error in *J* value measurements is ±1 Hz.

DISCUSSION

Dependence of the Solution Conformation of the Dodecamer on the Concentration of Ammonia. At low ammonia concentration, the dodecamer adopts in solution a B-type conformation. As shown in Figure 2, the interresidue *n*H8/H6-(*n*−1)H2′ NOESY cross-peaks are less intense than the intraresidue *n*H8/H6-*n*H2′ cross-peaks for all bases (except the terminal C1). This indicates that the intraresidue distances *n*H8/H6-*n*H2′ are shorter than the interresidue ones, a characteristic feature of B-type DNA (Van de Ven & Hilbers, 1988). Further evidence for the B-type conformation of the dodecamer is provided by the DQF-COSY results. As shown in Table 1, for all residues (except terminal G12), the $^3J_{H1'-H2''}$ values (5.0−6.3 Hz) are smaller than the $^3J_{H1'-H2'}$ values (8.7−9.9 Hz). Moreover, no H2″-H3′ cross-peaks were observed, except for terminal C1 and G12. These two findings limit the deoxyribose pseudorotation phase angle, P, to values between 110° and 180° (Hosur et al., 1986). This range includes the C2′-endo conformation characteristic of B-type DNA (P = 162°) and excludes the C3′-endo conformation (P = 18°) that is observed in A-type DNA. The pattern of intensities of DQF-COSY cross-peaks between H3′ and H4′ protons allowed further definition of sugar geometries. In the DQF-COSY spectra, the region containing H3′-H4′ connectivities is less affected by the signal from residual water than in NOESY spectra. This is due to the fact that the DQF-COSY pulse sequence suppresses singlet resonances in the spectrum (Piantini et al., 1982), and thus, the signal from residual water is reduced. The H3′-H4′ cross-peaks of C3, T7, and C8 were strong, suggesting a value of *P* close to 126°, i.e., C1′-exo conformation of deoxyribose (data not shown). The H3′-H4′ cross-peaks of G5, A6, and T9 were weaker, and those of G2 and A4 were hardly seen, indicating that the sugar conformations in these nucleotides range between C1′-exo and C2′-endo ($120° < P < 160°$). No H3′-H4′ cross-peak was observed for G10, consistent with C2′-endo conformation ($P \approx 160°$) for this nucleotide.

Several findings in the present work indicate that the overall conformation of the dodecamer observed in 0.002 M ammonia buffer is preserved over the entire range of ammonia concentrations investigated. These findings are summarized as follows:

(i) In 0.5 M ammonia, the intensity pattern of the interresidue *n*H8/H6-(*n*−1)H2′ NOESY cross-peaks relative to the intraresidue *n*H8/H6-*n*H2′ cross-peaks is the same as that at low ammonia concentration (Figure 2).

(ii) The changes in chemical shift upon increasing ammonia concentration are small, not exceeding 0.1 ppm (Figure 4). They affect mostly the protons of nucleotides located in the central part of the dodecamer. The largest shifts are observed for the sugar protons of T7 and C8, e.g., T7-H3′ and C8-H1′.

(iii) Increasing ammonia concentration does not alter significantly the $^3J_{H1'-H2'}$ and $^3J_{H1'-H2''}$ coupling constants and the sums $\sum_{1'}$ ($= {}^3J_{H1'-H2'} + {}^3J_{H1'-H2''}$) (Table 1). Moreover, in 0.5 M ammonia, no H2″-H3′ cross-peaks were observed, and the intensity pattern of H3′-H4′ cross-peaks remained similar to that in 0.002 M ammonia (except that the very weak H3′-H4′ cross-peaks of G2 and A4 were not observed). All of these results support the conclusion that ammonia does not induce significant changes in the sugar geometry.

(iv) The variations observed in the NOESY cross-peak volumes (Figure 5) suggest that ammonia induces small changes in interproton distances. The relative changes in cross-peak volumes upon increasing ammonia concentration from 0.002 to 0.5 M are less than 150%. In a two-spin approximation, this corresponds to changes in interproton distances of 16% or less. Concerted changes occur for the interresidue *n*H8/H6-(*n*−1)H1′ cross-peaks (solid bars in upper panel in Figure 5): for all cross-peaks that can be resolved, the volumes increase by at least 50%. In parallel, the volumes of intraresidue *n*H8/H6-*n*H2′ cross-peaks decrease (solid bars in lower panel in Figure 5).

(v) The changes in ^{31}P chemical shifts are small (0.2 ppm or less; Figure 6C). The largest changes are observed for the resonance at −0.82 ppm and one of the resonances at −0.74 ppm (in 0.002 M ammonia) which, during the titration, shift by 0.1 and 0.2 ppm, respectively. These findings suggests that, upon increasing ammonia concentration, the torsional angles ω and ω' at two phosphate groups change toward a less extended conformation (e.g., g,t or g,g; Gorenstein, 1981). Identification of these phosphate groups awaits assignment of the ^{31}P resonances of the dodecamer.

Table 2: Relaxation Rates for Selected Protons in the Dodecamer in 0.002 and 0.5 M Ammonia Buffers at 15 °C

proton	ammonia concentration 0.002 M	ammonia concentration 0.5 M	ratio of relaxation rates at the two ammonia concentrations	
	(A) Transverse Relaxation Rates, T_2^{-1} (s^{-1})			
A4-H8	17 ± 2	27 ± 3		1.6 ± 0.2
A6-H8	19 ± 2	26 ± 3		1.4 ± 0.2
T7-H6	21 ± 2	35 ± 3		1.6 ± 0.2
T7-CH_3	13 ± 1	18 ± 2		1.4 ± 0.2
T9-CH_3	13 ± 1	18 ± 2		1.4 ± 0.2
			average:	1.49 ± 0.09
H_2O	22 ± 2	23 ± 2		1.1 ± 0.1
	(B) Longitudinal Relaxation Rates, T_1^{-1} (s^{-1})			
A4-H8	2.9 ± 0.1	4.3 ± 0.2		1.48 ± 0.09
A6-H8	3.8 ± 0.2	5.9 ± 0.3		1.6 ± 0.1
T7-H6	4.5 ± 0.2	6.3 ± 0.3		1.4 ± 0.09
T7-CH_3	1.5 ± 0.08	2.1 ± 0.1		1.4 ± 0.1
T9-CH_3	1.4 ± 0.07	1.9 ± 0.09		1.36 ± 0.09
			average:	1.45 ± 0.04
H_2O	0.110 ± 0.002	0.100 ± 0.002		0.91 ± 0.03
	(C) Cross-Relaxation Rates, R_{ij} (s^{-1})[b]			
C1 H5-H6	1.56 ± 0.06	2.20 ± 0.06		1.41 ± 0.07
C8 H5-H6	1.45 ± 0.03	2.02 ± 0.02		1.39 ± 0.03
C3 + C11 H5-H6[a]	1.33 ± 0.03	2.24 ± 0.04		1.68 ± 0.05
T7 H6-CH_3	0.37 ± 0.02	0.61 ± 0.05		1.6 ± 0.2
T9 H6-CH_3	0.46 ± 0.05	0.57 ± 0.07		1.3 ± 0.2
			average:	1.48 ± 0.06

[a] The two cross-peaks overlap. [b] Between pairs of protons.

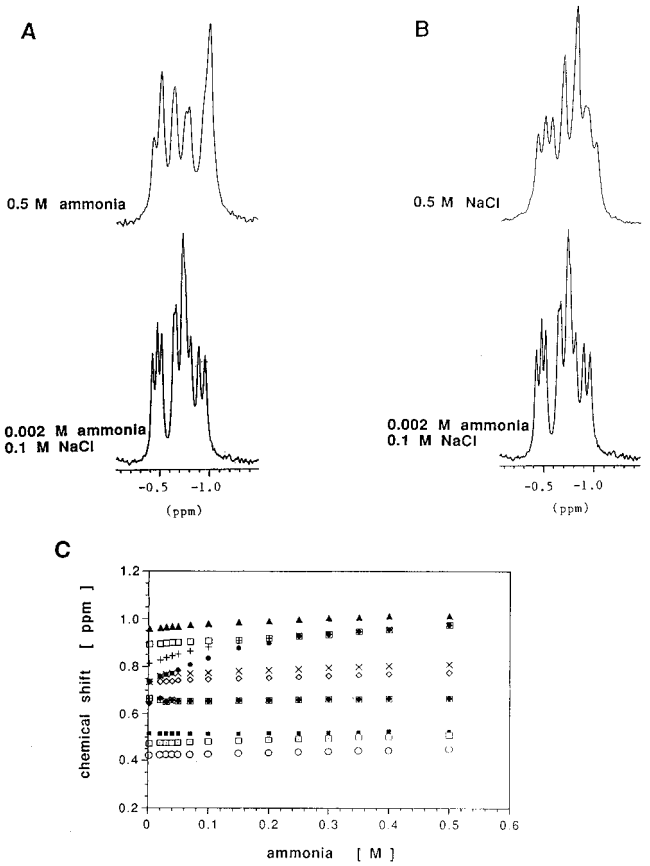

FIGURE 6: Effect of ammonia (A) and NaCl (B) upon the ^{31}P NMR spectra of the dodecamer at 15 °C. (C) Dependence of the chemical shift of ^{31}P NMR resonances of the dodecamer on ammonia concentration.

The remaining nine ^{31}P resonances are either constant during the ammonia titration or change by 0.05 ppm or less (Figure 6C). This fact indicates that the extrinsic effects on ^{31}P chemical shifts from changing solvent composition and from replacing Na^+ counterions by ammonium ions are small.

In summary, the changes in proton and phosphorus chemical shifts, NOESY cross-peak volumes and deoxyribose coupling constants over the range of ammonia concentration investigated suggest that ammonia induces subtle changes in the conformation of the dodecamer in solution. However, the overall structure of the dodecamer remains the same and is close to the B-type DNA structure.

Effect of Ammonia on Motional Properties of the Dodecamer. In contrast to the small structural changes described above, the changes in proton relaxation rates induced by ammonia are much larger. For all protons measured, longitudinal, transverse, and cross-relaxation rates are accelerated when ammonia concentration is raised from 0.002 to 0.5 M (Table 2). The fact that all relaxation rates increase suggests that the effect originates from an increase in the overall correlation time of the dodecamer at high ammonia concentration.

For homonuclear relaxation in the absence of paramagnetic species the auto- and cross-relaxation rates of a proton i (R_{ii} and R_{ij} in the relaxation matrix **R**, eq 1) are expressed as (Abragam, 1961)

$$R_{ii} = 0.1\gamma_H^4\hbar^2(\sum_j 1/r_{ij}^6)[J(0) + 3J(\omega_H) + 6J(2\omega_H)] \quad (3)$$

$$R_{ij} = 0.1\gamma_H^4\hbar^2(1/r_{ij}^6)[6J(2\omega_H) - J(0)] \quad (4)$$

Similarily, the transverse relaxation rate is

$$T_{2i}^{-1} = 0.05\gamma_H^4\hbar^2(\sum_j 1/r_{ij}^6)[5J(0) + 9J(\omega_H) + 6J(2\omega_H)] \quad (5)$$

where γ_H is the proton gyromagnetic ratio, $\hbar$ is Planck's constant divided by 2π, ω_H is the Larmor frequency, and r_{ij} is the distance between proton i and a neighboring proton j.

The spectral density, $J(\omega)$, for isotropic motion is given by

$$J(\omega) = \tau_c/(1 + \tau_c^2\omega^2) \quad (6)$$

where τ_c is the correlation time. For a DNA dodecamer at 15 °C the overall correlation time is of the order of 6 ns (Eimer et al., 1990) which, at a proton frequency of 400 MHz, corresponds to the slow motion limit ($\tau_c^2\omega^2 = 227 \gg 1$). Thus, neglecting any internal motions, the expressions for the relaxation rates can be simplified as

$$R_{ii}^{-1} = 0.1\gamma_H^4\hbar^2\tau_c\sum_j 1/r_j^6 \quad (7)$$

$$R_{ij} = -0.1\gamma_H^4\hbar^2\tau_c 1/r_{ij}^6 \quad (8)$$

$$T_{2i}^{-1} = 0.25\gamma_H^4\hbar^2\tau_c\sum_j 1/r_j^6 \quad (9)$$

In this limit, the auto- and cross-relaxation rates as well as the transverse relaxation rate depend linearly on correlation time, τ_c. In a multispin system such as the DNA dodecamer investigated, the longitudinal relaxation rate of a given proton in a selective saturation−recovery experiment (T_{1i}^{-1}, Table 2) depends on the auto- and cross-relaxation rates of other protons in the molecule. According to eqs 7 and 8, an increase in the correlation time should increase the R_{ii} and R_{ij} rates of all protons by the same factor. Then, as shown previously (Hull & Sykes, 1975), the observed T_{1i}^{-1} rate of the proton of interest should also increase.

As shown in Table 2, ammonia induces parallel changes in the transverse, longitudinal, and cross-relaxation rates. The changes in all these relaxation rates range from 30% to 68% with an average value of ∼50%. This suggests that the correlation time of the dodecamer increases by approximately 50% upon changing ammonia concentration from 0.002 to 0.5 M. Some of the observed changes in T_{1i}^{-1} and T_{2i}^{-1} may also result from changes in the distances between the proton of interest and its neighboring protons (r_{ij} in eqs 7 and 9). However, for pairs of protons in which the distance is independent of conformation, such as cytosine H5-H6 (interproton distance 2.46 Å), the cross-relaxation rates depend solely on the correlation time (eq 8). Then, based on the measured cross-relaxation rates (Table 2C), one can estimate that the correlation time of the dodecamer changes from ∼6 to ∼9 ns when ammonia concentration is increased from 0.002 to 0.5 M.

An alternative explanation for the changes in relaxation rates observed in the present work is that paramagnetic metal traces from the concentrated ammonia buffer may have been introduced into the DNA sample. To rule out this possibility, we have measured the longitudinal and transverse relaxation rates for the protons of the residual water in the two DNA samples used for relaxation measurements. As shown in Table 2, the relaxation of water protons is unaffected by ammonia, indicating that any paramagnetic contribution to the enhancement in the relaxation rates observed for the DNA protons is negligible.

Relevance of the Present Results for Measurements of Base-Pair Opening in DNA. Our observation that increasing ammonia concentration affects proton relaxation rates has important implications for measurements of the exchange rates of imino protons on the basis of NMR relaxation. In general, the observed longitudinal or transverse relaxation rates of imino protons in DNA, $1/[T_1]^{observed}$ or $1/[T_2]^{observed}$, respectively, contain contributions from proton dipolar interactions and from chemical exchange:

$$1/[T_{1(2)}]^{observed} = 1/[T_{1(2)}]^{dipolar} + k_{ex} \quad (10)$$

The chemical exchange contribution, k_{ex}, depends on the concentration of base catalyst, [B], and on the kinetics of base-pair opening. This dependence is expressed as

$$k_{ex} = k_{op}k_B[B]/(k_{cl} + k_B[B]) \quad (11)$$

where k_{op} and k_{cl} are the rate constants for opening and closing of the base pair, respectively, and k_B is the catalytic constant for abstraction of the imino proton by the base catalyst from the open state of the base pair. An alternative form of the same equation is (Leroy et al., 1985a)

$$\tau_{ex} = 1/k_{ex} = \tau_o + D[B]^{-1} \quad (12)$$

where $\tau_o = 1/k_{op}$ is the lifetime of the base pair in the closed state, and D is a constant defined as $(K_{op}k_B)^{-1}$ in which K_{op} is the equilibrium constant for formation of the open state of the base pair ($K_{op} = k_{op}/k_{cl}$). τ_o can be obtained as the limit of τ_{ex} at infinite concentration of base catalyst. The dipolar contribution to the relaxation rates ($1/[T_{1(2)}]^{dipolar}$ in eq 10) is usually assumed to be independent of the concentration of base catalyst.

In the present work we have shown that, upon increasing ammonia concentration, the relaxation rates of non-exchangeable protons increase, most likely due to an increase in the correlation time of the DNA molecule. These changes should affect also the dipolar contribution to the relaxation times of imino protons, $T_1^{dipolar}$ and $T_2^{dipolar}$. To understand how this effect may influence measurements of base-pair opening kinetics, we have simulated the dependence of longitudinal and transverse relaxation times on base catalyst concentration using eqs 10 and 12 (Figure 7). The values of the base-pair lifetime, τ_o, and constant D used in these calculations were those previously obtained for the guanine in position 10 in the dodecamer at 15 °C, namely, $\tau_o = 12.1$ ms and $D = 13.6$ M ms (Folta-Stogniew & Russu, 1994). The dipolar contributions to the observed relaxation rates were either held constant, $T_{1(2)}^{dipolar} = T_{1(2)}^0$, or assumed to depend linearly on the base catalyst concentration [B] as $T_{1(2)}^{dipolar} = T_{1(2)}^0(1 - 1.4[B])$, with $T_1^0 = 276$ ms and $T_2^0 = 33$ ms as previously determined (Folta-Stogniew & Russu, 1994). For the purposes of this illustration, the dependence of $T_{1(2)}^{dipolar}$ was chosen such that, at a base catalyst concentration of 0.2 M, the dipolar relaxation rates increase by 40%. As expected, the enhancement of dipolar relaxation by the base catalyst shortens the observed relaxation times (filled versus open symbols in Figure 7A and B). The effects are larger for the transverse relaxation time than for the longitudinal relaxation time, especially at high base concentrations. This is due to the fact that the dipolar component of transverse relaxation is almost an order of magnitude greater than that of longitudinal relaxation, e.g., $1/T_2^0 = 30$ s^{-1} and $1/T_1^0 = 3.6$ s^{-1} for the case shown in Figure 7. Thus, a fractional increase in dipolar relaxation of, for example, 40% has a larger effect on the value of the transverse relaxation rate than on that of the longitudinal relaxation rate.

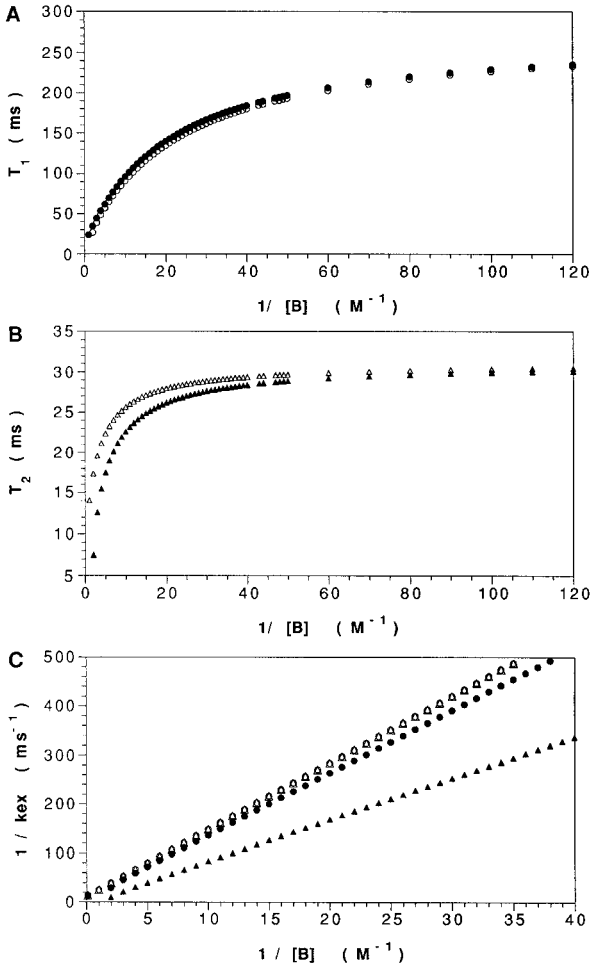

FIGURE 7: Theoretical curves showing the dependence of relaxation times and exchange times of a DNA imino proton on the inverse of base catalyst concentration. (A) Longitudinal relaxation time, T_1 (ms), calculated based on eqs 10 and 12 for $\tau_o = 12.1$ ms and $D = 13.6$ M ms. The open circles are T_1 values calculated assuming base-independent $T_1^{dipolar} = T_1^0 = 276$ ms, and the filled circles are T_1 values calculated assuming that $T_1^{dipolar}$ depends linearly on base concentration [B], as $T_1^{dipolar} = T_1^0(1 - 1.4[B])$. (B) Transverse relaxation time, T_2 (ms), calculated based on eqs 10 and 12 using the same values for τ_o and D as in panel A. The open triangles are T_2 values calculated assuming base-independent $T_2^{dipolar} = T_2^0 = 33$ ms and the filled triangles are T_2 values calculated assuming that $T_2^{dipolar}$ depends linearly on base concentration [B], as $T_2^{dipolar} = T_2^0(1 - 1.4[B])$. (C) Exchange times ($\tau_{ex} = 1/k_{ex}$) calculated from the T_1 and T_2 values shown in panels A and B based on eq 10. The symbols are the same as in panels A and B.

The ammonia-induced enhancement in dipolar proton relaxation affects imino proton exchange rates as illustrated in Figure 7C. In this figure, the exchange rates were calculated from the simulated curves for T_1 and T_2 (Figure 7A and B) based on eq 10. As usually done in the analysis of experimental imino proton exchange data, the term $T_{1(2)}^{dipolar}$ was taken as the asymptote of the $T_{1(2)}$ curves at low base concentrations [$T_{1(2)}^{dipolar} = T_{1(2)}^0$]. Clearly, the base-induced increases in the dipolar component of relaxation led to changes in the intercept and in the slope of $1/k_{ex}$ vs 1/[B], especially for values derived from T_2 measurements. According to eq 12, these changes result in an underestimation of the base-pair lifetime τ_o (smaller intercept) and an overestimation of the equilibrium constant for the formation of the open state of the base pair, K_{op} (smaller slope). They may even result in negative values for the base-pair lifetime (filled triangles in Figure 7C). Negative values for base-pair lifetimes have been previously reported for several DNA oligonucleotides (Benight et al. 1988; Plum & Bloomfield 1990). In these studies, imino proton exchange rates were calculated from changes in the line widths of imino proton resonances. The present analysis suggests that the negative lifetimes previously observed may have resulted from changes in the dipolar relaxation rate induced by the base catalyst.

In summary, our results indicate that imino proton exchange rates derived from measurements of proton relaxation rates can be affected by ammonia-induced increases in dipolar relaxation. The exchange rates derived from transverse relaxation rates can be corrected for this effect by measuring, for example, the changes in resonance line width for non-exchangeable protons induced by the base catalyst. The exchange rates calculated from longitudinal relaxation rates could be corrected in a similar manner, although the present analysis suggests that they are less affected by ammonia-induced changes in the dipolar relaxation.

Molecular Origin of the Ammonia-Induced Increase in the Correlation Time of the DNA Dodecamer. The molecular processes that could contribute to an increase in the DNA correlation time at high ammonia concentrations are not fully understood. The change in the viscosity of water in the presence of ammonia is not large enough to account for the observed increase in the DNA correlation time: the viscosity of a 0.5 M ammonia solution differs from that of water only by 1%, and that of a 0.5 M ammonium chloride solution (which forms due to the titration of the buffer to pH 8.9) differs from that of water by only 2% (Weast, 1986). The interactions of ammonium ions with the DNA may be expected to affect the effective hydrodynamic volume of the molecule due to changes in the nature of counterions and/or changes in hydration. Alternatively, the effect of ammonia may be nonspecific and may simply result from the high ionic strength associated with high ammonia concentrations. In order to distinguish between ammonia-specific and nonspecific ionic effects we have investigated the effects of NaCl upon the ^{1}H and ^{31}P spectra and proton relaxation in the dodecamer. The DNA sample in 0.002 M ammonia buffer (containing 100 mM NaCl and 2 mM EDTA in D_2O) was titrated to 0.5 M NaCl by addition of NaCl from a stock solution (4 M NaCl in 0.002 M ammonia buffer with 2 mM EDTA, pH-meter reading 8.9). As shown in Figures 8 and 6B, in 0.5 M NaCl significant broadening of the ^{1}H and ^{31}P resonances of the dodecamer is observed. The longitudinal relaxation rates of A4-H8, A6-H8, T7-H6, T7-CH_3, and T9-CH_3 protons also increase upon increasing NaCl concentration, and the changes are comparable to those observed in 0.5 M ammonia (data not shown). These results suggest that the high ionic strength associated with high ammonia concentrations contributes to the increase in the DNA correlation time, possibly by inducing intermolecular association of the DNA dodecamers. This suggestion is consistent with previous observations that DNA and RNA oligomers at milimolar concentration are prone to end-to-end aggregation when exposed to high concentrations of NaCl (Patel & Canuel, 1979; Borer et al., 1975; Kochoyan et al., 1987). Higher concentrations of NaCl do not affect significantly the spectral positions of the ^{31}P resonances of the dodecamer (Figure 6B). Moreover, in ^{1}H spectra, the

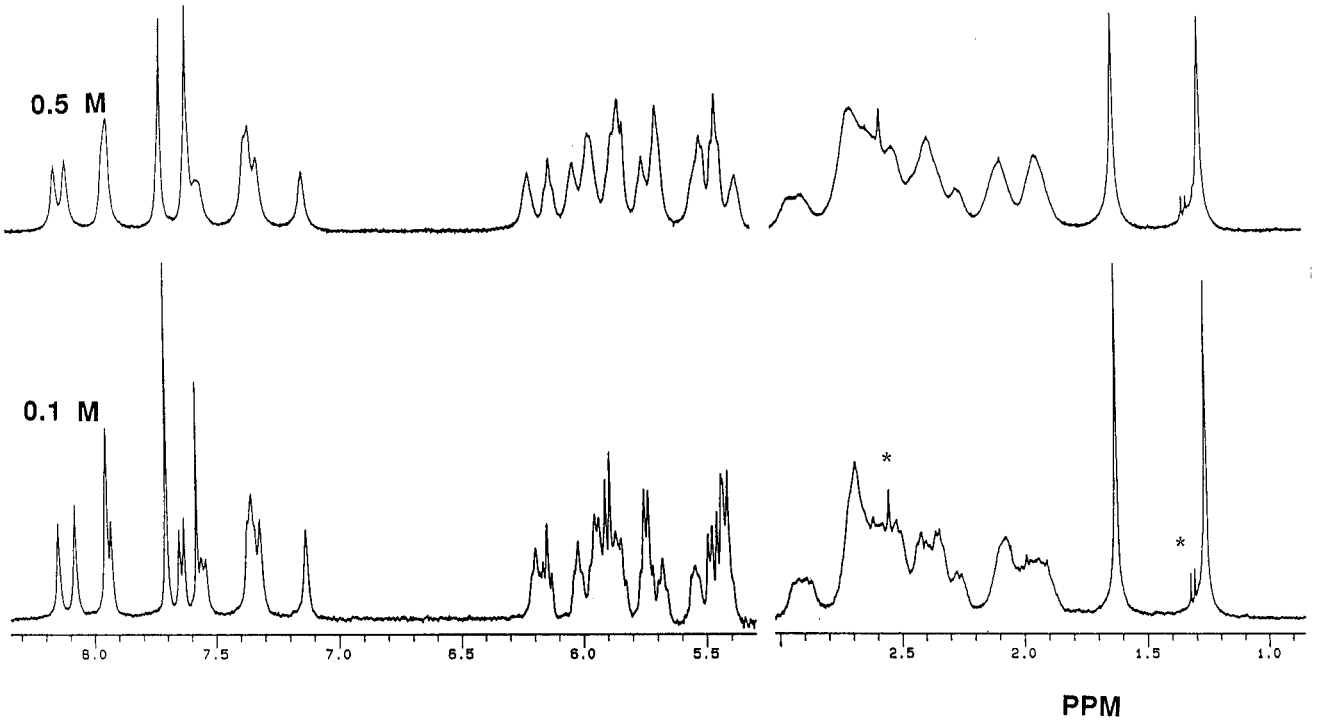

FIGURE 8: Selected regions of the ^{1}H NMR spectra of the dodecamer in 0.1 and 0.5 M NaCl, at 15 °C. Solution conditions: 0.002 M ammonia buffer in D_2O with 2 mM EDTA, pH-meter reading 8.9 (at 25 °C). The resonances indicated by the asterisk originate from an impurity in the buffer.

chemical shifts of only a few resonances are changing upon increasing NaCl concentration (Figure 8). For example, in the aromatic proton resonance region, only the H6 resonance of the terminal cytosine in position 1 (7.63 ppm) moves significantly upfield upon addition of NaCl, consistent with end-stacking of the dodecamer molecules at higher concentrations of NaCl.

In contrast to NaCl, increasing concentrations of ammonia change the chemical shift of a larger number of ^{1}H and ^{31}P resonances of the dodecamer (Figures 1, 4, and 6). In the present work, we have shown that these changes originate from subtle alterations in the DNA solution conformation. Thus, it appears that, in addition to inducing aggregation, ammonia ions may interact with the DNA in a more specific manner than NaCl. This suggestion is consistent with the results of Fazakerley et al. (1984) who detected by NMR a complex between ammonium ion and the hexamer $[d(GCGCGC)]_2$. This complex appeared to be sequence-specific since it was not observed for the hexamer $[d(GGATCC)]_2$.

CONCLUSIONS

Measurements of base-pair opening in DNA using imino proton exchange require high concentrations of exchange catalysts such as ammonia. The results presented in this paper demonstrate that, over the range of ammonia concentrations from 0.002 to 0.5 M, the overall solution structure of the DNA dodecamer investigated is preserved. However, high ammonia concentrations increase proton transverse, longitudinal, and cross-relaxation rates, most likely due to an increase in the DNA correlation time. The ammonia-induced changes in dipolar relaxation should be considered when using proton relaxation to measure imino proton exchange and base-pair opening kinetics in DNA.

REFERENCES

Abragam, A. (1961) *The Principles of Nuclear Magnetism*, p 295, Oxford University Press, London, U.K.

Benight, A. S., Schurr, J. M., Flynn, P. F., Reid, B. R., & Wemmer, D. E. (1988) *J. Mol. Biol. 200*, 377−399.

Borer, P. N., Kan, L. S., & Ts'o, P. O. P. (1975) *Biochemistry 14*, 4847−4863.

Cheung, S., Arndt, K., & Lu, P. (1984) *Proc. Natl. Acad. Sci. U.S.A. 81*, 3665−3669.

Early, T. A., Kearns, D. R., Hillen, W., & Wells, R. D. (1981) *Biochemistry 20*, 3756−3764.

Eimer, W., Williamson, J. R., Boxer, S. G., & Pecora, R. (1990) *Biochemistry 29*, 799−811.

Englander, S., W., & Kallenbach, N. R. (1984) *Q. Rev. Biophys. 16*, 521−655.

Fazakerley, G. V., van der Marel, G. A., van Boom, J. H., & Guschlbauer, W. (1984) *Nucleic Acids Res. 12*, 8269−8279.

Folta-Stogniew, E., & Russu, I. M. (1994) *Biochemistry 33*, 11016−11024.

Glasoe, P. K., & Long, F. A. (1960) *J. Phys. Chem. 64*, 188−190.

Gorenstein, D. G. (1981) *Annu. Rev. Biophys. Bioeng. 10*, 355−386.

Gueron, M., Kochoyan, M., & Leroy, J.-L. (1987) *Nature 328*, 89−92.

Gueron, M., Charretier, E., Hagerhorst, J., Kochoyan, M., Leroy, J. L., & Moraillon, A. (1990) *Structure & Methods* (Sarma, R. H., & Sarma, M. H., Eds.) Vol. 3, pp 113−137, Adenine Press, New York.

Hosur, R. V., Ravikumar, M., Chary, K. V. R., Sheth, A., Govil, G., Zu-Kun, T., & Miles, H. T. (1986) *FEBS Lett. 205*, 71−76.

Hull, W. E., & Sykes, B. D. (1975) *J. Chem. Phys. 63*, 867−880.

Kochoyan, M., Leroy, J. L., & Gueron, M. (1987) *J. Mol. Biol. 196*, 599−609.

Kochoyan, M., Leroy, J. L., & Gueron, M. (1990) *Biochemistry 29*, 4799−4805.

Leontis, N. B., & Moore, P. B. (1986) *Biochemistry 25*, 5736−5744.

Leroy, J. L., Broseta, D., & Gueron, M. (1985a) *J. Mol. Biol. 184*, 165−178.

Leroy, J. L., Bolo, N., Figueroa, N., Plateau, P., & Gueron, M. (1985b) *J. Biomol. Struct. Dyn. 2*, 915−939.
Leroy, J. L., Kochoyan, M., Huynh-Dinh, T., & Gueron, M. (1988) *J. Mol. Biol. 200*, 223−238.
Mandal, C., Kallenbach, N. R., & Englander, S. W. (1979) *J. Mol. Biol. 135*, 391−411.
Macura, S., & Ernst, R., R. (1980) *Mol. Phys.* 41, 95−117.
Moe, J. G., & Russu, I. M. (1990) *Nucleic Acids Res. 18*, 821−827.
Moe, J. G., & Russu, I. M. (1992) *Biochemistry 31*, 8421−8428.
Neuhaus, D., Wagner, G., Vasak, M., Kagi, J. H. R., & Wüthrich, K. (1985) *Eur. J. Biochem. 151*, 257−273.
Pardi, A., Morden, K. M., Patel, D. J., & Tinoco, I., Jr. (1982) *Biochemistry 21*, 6567−6574.
Patel, D. J., & Canuel, L. L. (1979) *Eur. J. Biochem. 96*, 267−276.
Patel, D. J., Ikuta, S., Kozlowski, S., & Itakura, K. (1983) *Proc. Natl. Acad. Sci. U.S.A. 80*, 2184−2188.
Piantini, U., Sorensen, O. W., & Ernst, R. R. (1982) *J. Am. Chem. Soc. 104*, 6800−6801.
Plum, G. E., & Bloomfield, V. A. (1990) *Biochemistry 29*, 5934−5940.
Rinkel, L. J., & Altona, C. (1987) *J. Biomol. Struct. Dyn. 4*, 621−649.
States, D. J., Haberkorn, R. A., & Ruben, D. J. (1982) *J. Magn. Reson. 48*, 286−292.
Teitelbaum, H., & Englander, S. W. (1975a) *J. Mol. Biol. 92*, 55−78.
Teitelbaum, H., & Englander, S. W. (1975b) *J. Mol. Biol. 92*, 79−92.
Van de Ven, F. J. M., & Hilbers, C. W. (1988) *Eur. J. Biochem. 178*, 1−38.
Weast, R. C., Ed. (1986) *CRC Handbook of Chemistry and Physics*, 67th ed., CRC Press, Boca Raton, FL.

BI952932Z